# Phase Separation on an Atomic Scale: The Formation of a Novel Quasiperiodic 2D Structure

J. E. Demuth, U. K. Koehler,[a] R. J. Hamers, and P. Kaplan
*IBM Research Division, Thomas J. Watson Research Center, Yorktown Heights, New York 10598*
(Received 22 August 1988)

Scanning tunneling microscopy of a "5×5"-Cu/Si(111) ordered layer reveals an unusual type of quasiperiodic phase. Topographic and spectroscopic images together with their Fourier analysis reveal at least three electronically and structurally distinct local phases which arrange to form a quasiperiodically ordered structure. The nature and origin of this novel structure is discussed.

PACS numbers: 68.65.+g, 61.16.Di

The initial ordering of lattice-mismatched systems has attracted wide attention. In numerous studies of weakly interacting systems this leads to incommensurate layers which exhibit locally ordered structures separated by domain walls.[1-3] Strongly interacting systems have been less widely studied, can be more complex,[4] and are important in understanding the initiation of epitaxial growth on semiconductor surfaces. Here we present new scanning-tunneling-microscopy (STM) results for Cu on Si which not only provides new insight into stress relief in such strongly interacting systems but illustrates a powerful, yet unexploited method, to analyze STM data. From a detailed analysis of the Fourier components of topographic and spectroscopic STM images, we identify the local origin of the unusual diffraction features in the "5×5"-Cu/Si system.[5,6] We also show that this strongly interacting system consists of at least three structurally and electronically distinct local phases which are quasiperiodically arranged on an atomic scale. The resulting structure is locally commensurate and analogous in many ways to the Si(111)-7×7 phase.

These experiments were performed in a UHV system designed for epitaxy and growth studies which allows *in situ* metal deposition and characterization by LEED, Auger, and STM.[7] *I-V* spectra were acquired at each pixel of a topographic scan and later analyzed as *I-V* spectra or current image tunneling spectroscopy (CITS) images.[8,9] A "5×5"-Cu/Si(111) structure was grown by deposition of 1.5 monolayers (ML) of Cu (as calibrated by a quartz-crystal monitor and Rutherford backscattering) onto a clean Si(111)-7×7 surface held at 620°C. As previously found, this structure is completed at 1.3 ML,[5] exists over a wide range of coverages (0.8–2 ML),[5,6,10] and produces a characteristic LEED pattern.[5,6] This pattern, while historically labeled as "5×5," contains both $\frac{1}{5}$- and $\frac{1}{6}$-order components, and is neither a 5×5 nor 6×6 structure.[5] Recent STM topographs have revealed the irregular nature of this structure and noted bias dependent images which prohibited a detail interpretation.[10]

In Fig. 1 we show a large-area STM topography together with a smaller region taken with a 1-nA tunneling current and +2-V sample bias. The image shows a variety of local structures which are labeled as deep craters (A), shallow craters (B), irregular islands (I), flat, triangular islands (T), as well as stripped regions (S). The T islands show a corrugation of 0.3 Å, the A craters show a 0.06-Å corrugation, and the strips S show a 0.03-Å corrugation. Both craters tend to have a triangular shape with an elevated central region while the strips, as noted elsewhere,[10] tend to line up to form bands across the surface. A Fourier analysis of this complex image, together with our spectroscopic data, allow us to understand the diffraction pattern[5,6] and nature of this "5×5" structure.

The Fourier components of this 2D image can be

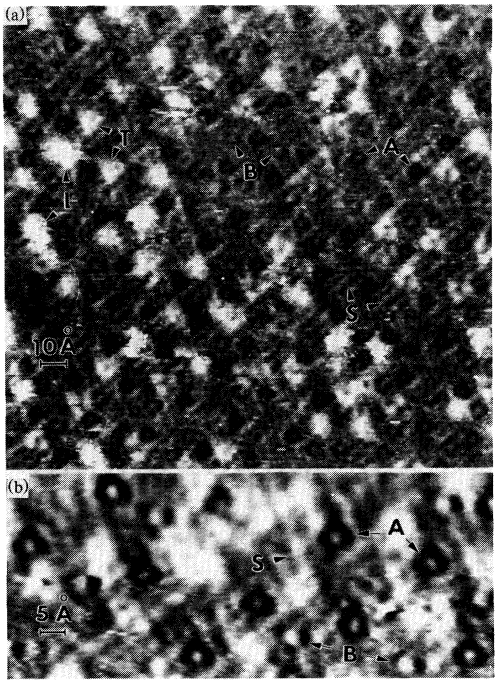


FIG. 1. Unfiltered STM topograph of (a) a 175×175-Å$^2$ area of a "5×5"-Cu/Si surface and of (b) a higher-resolution section, both obtained with a +2-V sample bias. The piezoelectric drift is uniform and uncorrected in both images.

directly compared to the reciprocal-lattice vectors determined in diffraction by our plotting the power spectrum[11] of the 2D Fourier transform (2D-FT PS). The 2D-FT PS for a 250×250-Å$^2$ scan is schematically shown in Fig. 2(a) and has been corrected for drift to produce the expected orientational symmetry. The overall sixfold-symmetric pattern is similar to that seen in LEED[5,6] and can be derived from the three wave vectors **q**, **s**, and **t** indicated in Fig. 2(a). This correspondence is significant since it means that the charge densities sampled here by STM have the same periodic components as the ion cores sampled in LEED, and that we are not neglecting features because of our choice of bias voltage. We also use the *relative* spot positions along the symmetry directions[5] and the characteristic pattern of spots between the arrows[6] to identify the Si(111) (10) and (01) reciprocal-lattice vectors which correspond here to the **s** wave vectors. This provides us with a more accurate value for **s** of 1.89 Å$^{-1}$ than is generally possible in real space due to uncertainties from the calibration, creep, or thermal drift of the piezoelectric scanner.

The amplitude profile of the 2D-FT PS along the (10) direction is shown in Fig. 2(b) and agrees with previous measurements.[5] This also reveals that **s** and **t** are noninteger values of **q** and that $\mathbf{q}\neq\mathbf{t}-\mathbf{s}$. Averaging all our data over equivalent symmetry directions, we find $\mathbf{t}=0.814(\pm 0.002)\mathbf{s}$, in agreement with LEED,[6] and $\mathbf{q}=\mathbf{s}/5.55$. As we next discuss, the **s** and **t** wave vectors can be associated with two different local structures where **q** arises from a disordered arrangement of these structures and not from a simple incommensurate phase.

The origin of these periodic components can be understood from the 2D-FT PS of selected features in the image. For example, choosing an appropriate intensity cutoff in the topographic image and setting the image to a uniform value for all points below or above this, allows us to examine the Fourier components of just the craters or I and T islands, respectively. We find that the distribution of the "craters" produces the strong set of Fourier components with only the **q** wave vectors inside the dashed ring shown in Fig. 2(a). The A features can be readily used to define irregular unit cells, hereafter called quasicells, which on average produce the **q** wave vectors. A section of a topograph and the corresponding quasicells are shown in Figs. 3(a) and 3(b), respectively. The B features indicated here by the dashed circles are always formed on one side of these quasicells while the T features, when they arise, occur on the other side. We attribute the T and I features to our use of higher coverages and the subsequent nucleation of other structures discussed elsewhere.[5,6,12] In the following we focus on this initial "5×5" structure.

To determine the locations of the periodic components which give rise to **t** and neighboring **q** wave vectors seen in Fig. 2(a), we back transform all equivalent **t** and $\mathbf{t}\pm\mathbf{q}$ Fourier components while maintaining their original phase information. This type of image reconstruction indicates the *overall* locations of these periodic components and is shown in Fig. 3(c). These **t** Fourier components are strongest near the A and B features and form a network between them characteristic of a domain wall or discommensuration.[4] The issue of whether this network reflects strained bonds or new local structures is

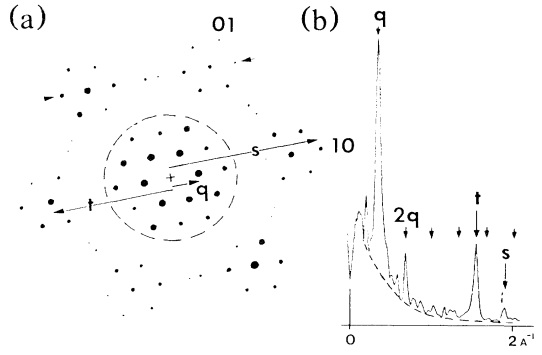


FIG. 2. (a) Schematic of the power spectrum of the 2D Fourier transform of a 6.25×10$^4$ Å$^2$ topographic scan where the diameter of the solid circles or points reflect relative intensities. The asymmetries in intensities can be associated with local irregularities and the finite area sampled. (b) The intensity profile of the power spectrum along the 10 direction. The small arrows mark the positions of the $n$**q** wave vectors and the dashed line near **s** marks the position of **t**+**q**.

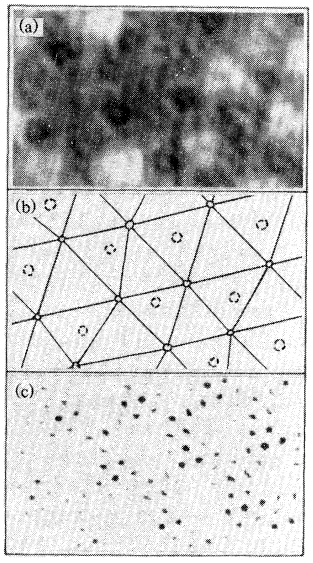


FIG. 3. (a) A section of drift-corrected, smoothed data (1 nA, +2 V), together with (b) a schematic of the quasicells. (c) The back transform of only the **t** and **t**+**q** Fourier components derived from a larger area but shown for this same area. Note that this back transform image is a "negative" where the stronger Fourier components are darker.

central to the understanding of the nature of the "5×5" phase. To resolve this, we must also consider the locations of the **s**-wave-vector components as well as their local electronic structure.

We find that the **s** Fourier components of the surface order are strongest at low bias and can be directly observed in the CITS spectroscopic images. In Figs. 4(a), 4(b), and 4(d), we show CITS images characteristic of different biases together with a corresponding schematic in 4(c) showing the location of the A, B, and S features. These structures all appear to be in registry with the 1×1 lattice of bulk terminated Si, obtained by back transforming all equivalent (01) and (10) Fourier components. The S features appear independent of bias and lie on one side of the quasicell while the B features are strongly bias dependent and lie on the other side of the quasicell. (We also note a second infrequent type of B phase which is not discussed.) While all regions on this surface show (atomically resolved) metallic *I-V* spectra

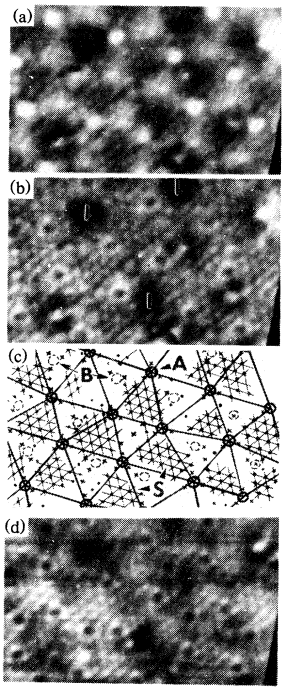


FIG. 4. Averaged spectroscopic CITS (Refs. 9 and 10) images representative of different energy ranges: (a) +1.4 to +1.2 V, (b) +0.06 to +0.4 V, and (d) −0.4 to −1.8 V. The schematic in (c) depicts various features discussed in the text. Here, the solid and dashed circles along with the surrounding features correspond to the A and B phases, respectively, and the dots forming the S region lie on the indicated 1×1 grid. [For these data we note that the tip is blunter than in Fig. 1 or 3. This reduces all corrugations in the simultaneously obtained topograph (1 nA, +2-V sample bias) and prohibits us from seeing the stripped features in the topograph.]

characteristic of a silicide,[13] several other states are observed for these different regions which produce the strong differences in the CITS images. The S region shows stronger tunneling for the occupied states than either the A or B regions and has an additional filled state near −1.2 eV. The empty states of the A and S regions show similar tunneling but differ markedly from B which has an additional empty state and more tunneling above +0.8 eV. Such electronic differences, together with the different local spacings in the A and B regions discussed earlier, imply that they are chemically different silicides than occur in the S region. The formation of such different local phases can be viewed as the decomposition of a single incommensurate phase into at least three phases which are in registry with the underlying lattice. The S, A, and B local structures fit together to form a "tiling" and define the irregular unit cells of this 2D lattice. We note that the meandering boundaries of these quasicells and the resulting nonintegral wave vectors are general properties of a quasicrystal.[14] The irregular locations of the A and B structures can be associated with a slight randomization of these local structures.

Although the topographic and spectroscopic features are suggestive of some specific models for these phases, such models are not unique. We instead discuss the likely physical origin of the "5×5" phase. The S-region silicide is coincident with the substrate and likely under severe stress due to the incorporation of Cu into the Si(111) lattice.[15] The strain is sufficiently strong so that ~2 surface lattice constants away from the center of the S region, a second phase A forms with a different arrangement of atoms (possibly even missing atoms). This A phase is analogous to the corner holes of Si(111)-7×7 which contribute to reduce strain energy.[16] In most cases the S phase extends across the quasicell and rules out the existence of a stacking fault as arises for Si(111)-7×7.[8,16] Without a stacking fault, the misfit eventually produces large stresses on the other side of the quasicell which leads to the B phase. The variations in the location of the A and B phases may reflect the small energy differences and weak long-range interactions between these phases. We also note that these variations are consistent with the absence of a stacking fault which on Si(111)-7×7 forces an alignment of the corner holes.

In general, the reduced coordination and ability to form new phases at surfaces may allow strongly interacting, strained surface layers to phase separate and produce this type of quasiperiodic, higher-order commensurate structure. We anticipate that the detailed behavior of this system will be useful in understanding surface ordering and stress relief in other strongly interacting, lattice-mismatched systems.

The authors are pleased to acknowledge useful discussions with D. DiVincenzo, R. Tromp, P. Horn, T. Hashizume, and Professor T. N. Rhodin (who brought this system to our attention), as well as the Office of Naval

Research for partial support of this work.

---

[a]Present address: Institut für Festkörperphysik, University of Hannover, Hannover, West Germany.

[1]J. P. McTague and A. D. Novaco, Phys. Rev. B **19**, 5299 (1979).

[2]Tetsuya Aruga, Hiroshi Tochihara, and Yoshitada Murata, Phys. Rev. Lett. **52**, 1794 (1984).

[3]Jinhe Cui, S. C. Fain, Jr., H. Freimuth, W. Wiechert, H. D. Schildberg, and H. J. Lauter, Phys. Rev. Lett. **60**, 1848 (1988).

[4]P. Bak, Rep. Prog. Phys. **45**, 587 (1982).

[5]E. Daugy, P. Matheiz, F. Salvan, and J. M. Layet, Surf. Sci. **154**, 267 (1985).

[6]K. Kemmann, F. Mueller, and H. Neddermeyer, Surf. Sci. **192**, 11 (1987).

[7]J. E. Demuth, E. J. van Loenen, R. M. Tromp, and R. J. Hamers, J. Vac. Sci. Technol. B **6**, 18 (1988).

[8]R. J. Hamers, R. M. Tromp, and J. E. Demuth, Phys. Rev. Lett. **56**, 1972 (1986).

[9]J. E. Demuth, R. J. Hamers, and R. M. Tromp, in *Interfaces, Superlattices, and Thin Films,* edited by J. D. Dow and I. K. Schuller, MRS Symposium Proceedings No. 77 (Materials Research Society, Pittsburgh, PA, 1987), p. 1.

[10]R. J. Wilson, S. Chiang, and F. Salvan, Phys. Rev. B **38**, 12696 (1988).

[11]The power spectrum $P$, of the Fourier transform $T_F$, is defined as $P=[(\mathrm{Re}T_F)^2+(\mathrm{Im}T_F)^2]^{1/2}$.

[12]St. Tosch and H. Neddermeyer, in Proceedings of the Third International Conference on Scanning Tunneling Microscopy, Oxford, United Kingdom, July 1988 (to be published).

[13]We note that the $I$-$V$ spectra and tunneling characteristics seen here are similar to those that we have found for $Pd_2Si$ and $CoSi_2$ silicide surfaces (unpublished).

[14]See, for example, D. R. Nelson and Bertrand Haperin, Science **229**, 223 (1985), and references therein.

[15]Angle-resolved photoemission and calculations by D. D. Chambliss, T. N. Rhodin, and R. V. Kasowski [J. Vac. Sci. Technol. A **6**, 1499 (1988)] indicate Cu $d$-band dispersions characteristic of Cu substituted for Si in a $1\times1$ lattice.

[16]R. M. Tromp and E. J. van Loenen, Surf. Sci. **155**, 432 (1985).

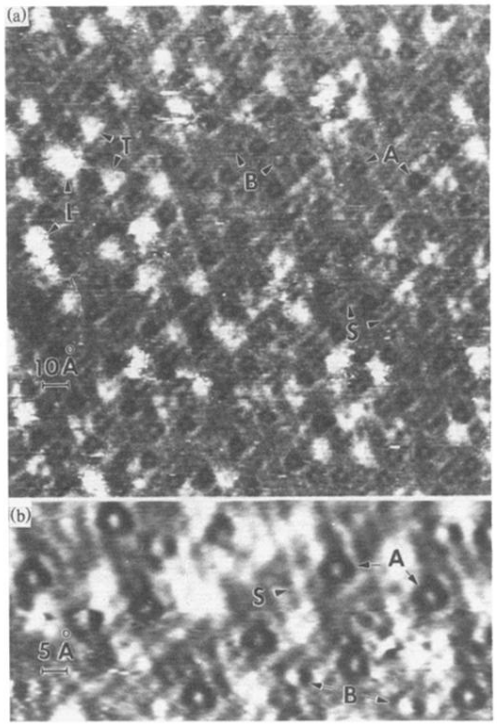


FIG. 1. Unfiltered STM topograph of (a) a 175×175-Å$^2$ area of a "5×5"-Cu/Si surface and of (b) a higher-resolution section, both obtained with a +2-V sample bias. The piezoelectric drift is uniform and uncorrected in both images.

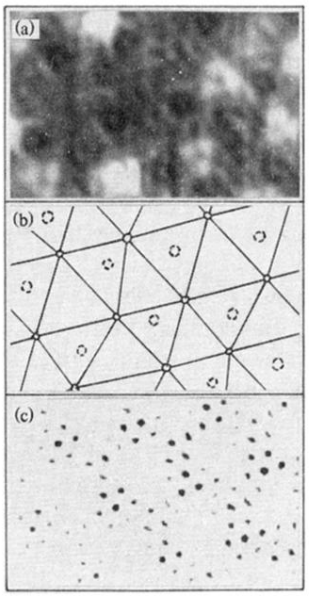


FIG. 3. (a) A section of drift-corrected, smoothed data (1 nA, +2 V), together with (b) a schematic of the quasicells. (c) The back transform of only the **t** and **t**+**q** Fourier components derived from a larger area but shown for this same area. Note that this back transform image is a "negative" where the stronger Fourier components are darker.

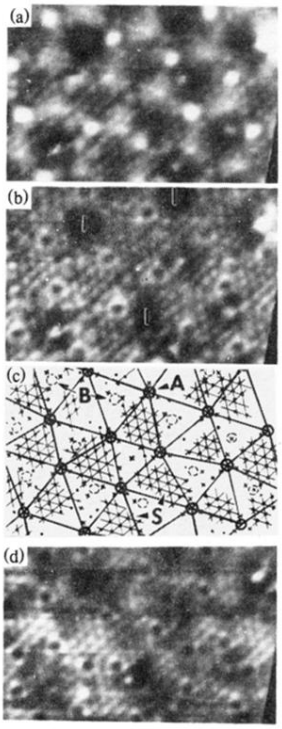


FIG. 4. Averaged spectroscopic CITS (Refs. 9 and 10) images representative of different energy ranges: (a) +1.4 to +1.2 V, (b) +0.06 to +0.4 V, and (d) −0.4 to −1.8 V. The schematic in (c) depicts various features discussed in the text. Here, the solid and dashed circles along with the surrounding features correspond to the A and B phases, respectively, and the dots forming the S region lie on the indicated 1×1 grid. [For these data we note that the tip is blunter than in Fig. 1 or 3. This reduces all corrugations in the simultaneously obtained topograph (1 nA, +2-V sample bias) and prohibits us from seeing the stripped features in the topograph.]